JME
Journal of Mechatronics Engineering

Ultrashort pulses propagation through different approaches of the Split-Step Fourier method

José Stênio de Negreiros Júnior[1], Daniel do Nascimento e Sá Cavalcante[1], Jermana Lopes de Moraes[2], Lucas Rodrigues Marcelino[1], Francisco Tadeu de Carvalho Belchior Magalhães[1], Renata Rodrigues Barboza[1], Marcos Lúnciel Rocha Menezes de Carvalho[1], Glendo de Freitas Guimarães[1]

[1]Photonics Laboratory, Federal Institute of Ceará (IFCE), Fortaleza, Brazil
[2]Graduate Program in Telecommunication Engineering, Federal Institute of Ceará (IFCE), and Federal University of Ceará (UFC), Fortaleza, Brazil

<steniojuniorsb@gmail.com>, <danielsacavalcante@gmail.com>, <jermanalopes@gmail.com>, <lucasrmarc@gmail.com>, <carvalho.tadeu@gmail.com>, <renatarodriguesbarboza@gmail.com>, <amarcoslunciel@gmail.com>, <glendodefreitas@gmail.com>

DOI: 10.21439/jme.v1i3.20

Received: 28 Nov. 2018. **Accepted:** 10 Dec. 2018

Abstract. Simulating the propagation of optical pulses in a single mode optical fiber is of fundamental importance for studying the several effects that may occur within such medium when it is under some linear and nonlinear effects. In this work, we simulate it by implementing the nonlinear Schrödinger equation using the Split-Step Fourier method in some of its approaches. Then, we compare their running time, algorithm complexity and accuracy regarding energy conservation of the optical pulse. We note that the method is simple to implement and presents good results of energy conservation, besides low temporal cost. We observe a greater precision for the symmetrized approach, although its running time can be up to 126% higher than the other approaches, depending on the parameters set. We conclude that the time window must be adjusted for each length of propagation in the fiber, so that the error regarding energy conservation during propagation can be reduced.

Keywords: Split-step Fourier Method. Ultrashort pulse propagation. Nonlinear Schrödinger Equation. Optical fiber. Nonlinear effects. Photonics.

1 Introduction

In the twentieth century, after the discovery of the first, second and third low loss and low dispersion windows in optical fibers, achieving an attenuation coefficient of less than 0.2 dB/km at the wavelength of 1550 nm (RIBEIRO, 2003), researchers initiated studies of ultrashort pulse propagation in optical fiber under linear dispersive effects and nonlinear effects (AGRAWAL, 2001).

The propagation of an optical pulse in a nonlinear optical fiber is mathematically represented by the Nonlinear Schrödinger Equation (NLSE). It is fundamentally important to do a numerical approximation, in order to improve the understanding of nonlinear effects in optical fibers, since the NLSE is a nonlinear partial differential equation, for which analytical solutions are possible only in a few cases (AGRAWAL, 2001). We searched in literature for the most recent studies on this topic, and the main results we have found are discussed next.

A widely used method to solve the problem of pulse propagation in non-dispersive and nonlinear media is the Split-Step Fourier method (SSFM), which is based on the Fast Fourier Transform (FFT) algorithm (KEISER, 2000). The SSFM is one of the most effective fi-

nite differences methods to solve the problem of NLSE, usually faster than most of the other finite difference methods, which is due to the fact that the implementation of the SSFM algorithm uses the Fourier transform as a basis (KOMNINOS, 2010). The choice of the method for solving the NLSE depends on the problem under analysis. The SSFM works efficiently when we intend to simulate a long link, but it does not provide satisfactory results for fiber Bragg gratings modeling, for instance (WASHBURN, 2002).

The precision of the SSFM may vary depending on the input parameters. There are various approaches for step-size controlling. Some researchers Balac & Mahé (2015) present a new method for estimating the local error in the S-SSFM when solving the NLSE, based on the step-doubling approach, but with less computational cost. Similarly, other authors Shao, Liang & Kumar (2014b) propose a scheme of adaptive step size combining the local error method and minimum area mismatch, which changes the step size depending on the local error of the current step, thus improving accuracy. Liu (2009) proposes an adaptive algorithm that adjusts the step sizes for a better accuracy and decrease of computational time.

Bayindir (2015) proposes an approach called Compressive Split-Step Fourier Method, using a number of spectral components smaller than usual. After performing the time integration and using the compressive sampling algorithm, the signal is reconstructed with better efficiency. In Duo & Zhang (2016), the authors propose three different Fourier spectral methods, and compare their results for solving the fractional NLSE. The SSFSM (Split-Step Fourier Spectral Method) presents the most accurate results for studying the behavior of the plane wave solutions. Taylor (2015) uses both SSFM and Finite Difference method to analyze the Soliton collision of a type of NLSE and compare their results, which show the SSFM is more stable, faster and can solve the equation on a larger spatial interval using a larger time step.

Although quite a lot of related work can be found in literature, we noticed that, so far, none of them has compared the running time of the SSFM in its various approaches, and none of them has studied the influence of the time window width regarding accuracy.

Therefore, in this paper, we analyze the implementation of the Split-Step Fourier method in some of its variations applied to the problem of propagation of an ultrashort optical pulse along a single mode fiber under the linear effects of second order dispersion and nonlinear effects of self-phase modulation (SPM). We compare the results obtained by each approach and analyze the running time, algorithm complexity and accuracy regarding energy conservation of the optical pulse in different variations of the method, and then we discuss the different parameters of the method, which must be adjusted for each scenario.

2 Theoretical Framework

2.1 Split-Step Fourier method

As the NLSE for the propagation of a pulse in optical fiber is a nonlinear partial differential equation, it only admits analytical solutions for a few and very specific problems. Thus, a numerical approach is necessary for a better understanding of nonlinear effects in optical fibers. Among the various finite differences and pseudo-spectral methods, we highlight the Split-Step Fourier method, due to its speed and accuracy (KEISER, 2000).

Generally, both linear and nonlinear effects occur simultaneously, so that we have to apply and analyze the two operators simultaneously. However, the SSFM operates with an approximated solution, assuming that when the optical pulse is propagated through a tiny distance, the effects of linearity and nonlinearity may be taken independently (KOMNINOS, 2010). Mathematical terms of dispersion and nonlinearity are separated and dissociated in NLSE, allowing the use of the SSFM to solve it (MUSLU; ERBAY, 2005).

In the SSFM, the fiber is divided into segments along its length, called steps (h), and the electromagnetic field is propagated in each segment considering linear and nonlinear effects, separately, as illustrated in Figure 1. We solve the linear equations directly in the frequency domain, whereas the nonlinear equations are solved within the time domain.

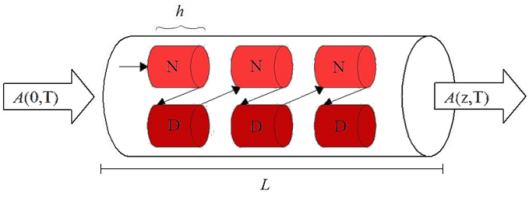

Figure 1: Example of pulse propagation with the traditional Split-Step Fourier Method.

From Figure 1, we notice that the propagation is performed at an initial z distance to the next distance

$(z + h)$ (GROSZ, 1998). The following equation shows the expression that determines such propagation.

$$A(z + h, T) = exp(hD)exp(hN)A(z, T) \quad (1)$$

where $A(z, T)$ corresponds to the pulse propagation in the previous step, and $A(z + h, T)$ represents the field after the step h. The terms D and N represent the dispersive parameter and nonlinear parameter, respectively.

The use of the Fourier transform makes the numerical calculation much faster, thus making the SSFM stand out regarding running time in comparison with other methods. The final equation of optical pulse propagation through the SSFM is represented by:

$$A(z + h, T) = \mathfrak{F}^{-1}\{exp(hD)\mathfrak{F}\{exp(hN)A(z, T)\}\} \quad (2)$$

After verifying Eq. 2, we can divide the implementation of the SSFM into four steps, as follows.

- **Step 1:** We analyze the nonlinear effects together with the pulse propagation function, since they are both in the time domain;
- **Step 2:** We calculate the Fourier transform of the output obtained in step 1, converting the pulse to the frequency domain, for linear effects analysis;
- **Step 3:** We apply the linear effects on the results of step 2, both in the frequency domain;
- **Step 4:** We calculate the inverse Fourier transform of step 3, returning the pulse to the time domain, and then returning to step 1.

2.2 Symmetrized split-step Fourier method

The accuracy of Split-Step Fourier method can be improved by using a derivation of this method, called Symmetrized Split-Step Fourier Method (S-SSFM). The concept of the S-SSFM is very similar to the SSFM, differing only in the way as the N and D operators are applied along the fiber (KOMNINOS, 2010).

In this method, the pulse is propagated up to half the step h considering the D operator, as shown in Figure 2(a). Then, the output of the D operator is used as input to the propagation along the entire step h with the N operator. Finally, the pulse is propagated along the other half the step h with the D operator, as shown

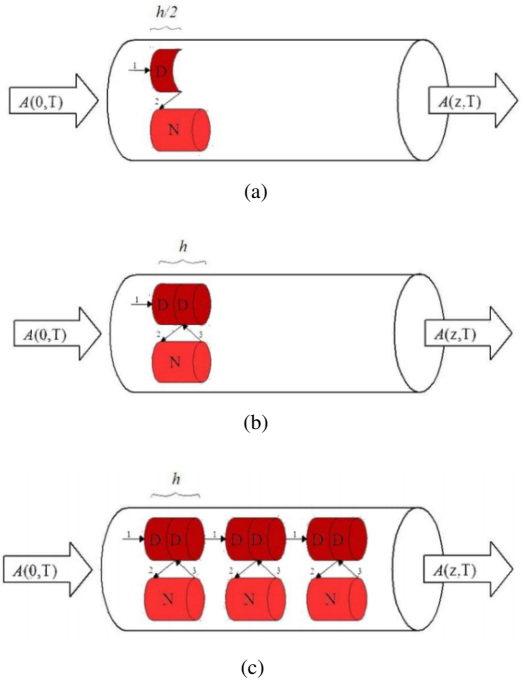

Figure 2: Schematic representations of S-SSFM.

in Figure 2(b). Then this process is repeated along the whole length of the fiber, as shown in figure 2(c).

Despite its better accuracy, the computational cost is higher since it is proportional to the number of FFTs performed (SHAO; LIANG; KUMAR, 2014a).

The expression that determines the S-SSFM is given by the equation 3 below

2.3 Numerical error

As previously mentioned, the SSFM calculates an approximation of the result of the NLSE. Therefore, there are factors that may influence the numerical error of the method. The choice of each parameter, such as step-size, temporal/spectral windows and other conditions of the pulse must be carefully adjusted in order to reach more accuracy. For instance, if we choose a wrong value for the spectral/temporal windows, there will be errors due to aliasing.

There are several papers that investigate the influence of the step-size on the energy conservation error and methods to minimize such error (BALAC; MAHÉ, 2015; ZHANG; LI; DONG, 2013; LIN et al., 2012; BALAC; FERNANDEZ, 2014; ZHANG; HAYEE, 2008). However, there is error inherent to the method itself due

$$A(z+h,T) = \mathfrak{F}^{-1}\left\{exp\left(\frac{h}{2}D\right)\mathfrak{F}\left\{exp\left(\int_{z}^{z+h} N(z')dz'\right)\mathfrak{F}^{-1}\left\{exp\left(\frac{h}{2}D\right)\mathfrak{F}\left\{A\left(z,T\right)\right\}\right\}\right\}\right\} \quad (3)$$

to the propagation of the D operator and the N operator separately, which does not happen in the real world.

3 Materials and Methods

The Split-Step Fourier method accepts some variations as for its implementation. The basis of the method consists in separating the dispersive linear effects (operator D), which occur in the frequency domain, and the nonlinear effects (operator N), which occur in the time domain, applying one operator at a time in each step h.

Traditionally, we first apply the N operator, since the pulse amplitude vector is initially in the time domain, and then, after applying the Fourier fast transform (FFT), we apply the operator D, then returning to the time domain through the application of the Inverse Fourier fast transform (IFFT) as shown in Table 1, with this variation code ($N - D$) implemented in MatLab.

Table 1: Split-Step Fourier Method N-D variation, implemented in MatLab.

```
for k = 1:h:L
  N = 1i*gama.*((abs(y)).^2);   %Nonlinear effects(NLE)
  y = exp(h.*N).*y;             %Application of NLE in the time domain
  y = fft(y);                   %Transformation to the frequency domain
  y = exp(h.*D).*y;             %Application of linear effects in the frequency domain
  y = ifft(y);                  %Transformation to the time domain
end
```

where h is the step size, L is the length of the fiber, gama is the nonlinearity parameter (γ) and y is the hyperbolic secant pulse.

Optionally, we can first apply the operator D and then the operator N, resulting in the variation $D-N$. In this case, the amplitude vector of the pulse is converted to the frequency domain using the FFT, then we apply the operator D, and after that we convert the pulse to the time domain through the application of the IFFT, and finally we apply the operator N, as shown in Table 2.

In order to reduce the error inherent to the method, we can also apply the S-SSFM. As shown in Table 3, the field is propagated only until half the step ($h/2$) with the operator D, then the resulting pulse is propagated along the entire step (h) with the operator N, and finally, the resulting field is propagated along the other half of the step ($h/2$) with the operator D.

Table 2: Split-Step Fourier Method D-N variation, implemented in MatLab.

```
for k = 1:h:L
    N = 1i*gama.*((abs(y)).^2);
    y = fft(y);
    y = exp(h.*D).*y;
    y = ifft(y);
    y = exp(h.*N).*y;
end
```

Table 3: Split-Step Fourier Method symmetrized variation, implemented in MatLab.

```
for k = 1:h:L
  N = 1i*gama.*((abs(y)).^2);
  y = fft(y);
  y = exp((h/2).*D).*y;
  y = ifft(y);
  y = exp(h.*N).*y;
  y = fft(y);
  y = exp((h/2).*D).*y;
  y = ifft(y);
end
```

In this paper, we compare the three variations regarding the error produced in the energy conservation and the running time for different values of input parameters. Then, we discuss the different parameters of the method, which must be adjusted for each scenario.

In the simulations with the three variations ($N - D$, $D - N$ and Symmetrized), we vary the length propagated (L), the step size (L) and the coefficient of nonlinearity (γ). As for the length propagated, we set the values of 1, 5 and 50 km. The step size (h) was varied according to a fixed number of steps (10, 50, 100, 500 and 1000 steps). As for the nonlinearity coefficient, we set the values of 0, 110^{-3}, 1010^{-3} and 10010^{-3} W^{-1}/km. Hence we have 15 scenarios for each value of nonlinearity coefficient. In all scenarios we work with 8192 points (window 8 times greater than that traditionally used in literature, 1024 points), initial pulse with time width of 2 ps, time window 200 times greater than the initial pulse (0,4 ns), group velocity dispersion coefficient of $\beta 2$ = -210^{-27} ps^2/km and initial power of 1 W. Besides, we set a null loss coefficient (α = 0) since we want to see the difference in energy conservation caused only by the error regarding the method.

We chose to represent the optical pulse with a great number of points in order to have an accurate representation of it, especially when under the nonlinear effect of self-phase modulation, which compresses the pulse, thus causing some power peaks. We also determined the size of the window in order to cover the whole width of the pulse after dispersion. Since the window in this method is cyclic (i.e., when the pulse exceeds an edge of the window it automatically penetrates through the other edge), there will be distortion of the pulse displayed if the window is not wide enough.

The simulations were performed on a computer with the following configurations: Intel(R) Core(TM) i5-2310 CPU @ 2.90 GHz, 2.9 GHz, RAM: 4 GB. During the execution, we closed all user processes, leaving only MatLab running for better precision as for running time. Additionally, for comparison, the same tests were performed on a laptop with the following configurations: Intel(R) Core(TM) i3-2330M CPU @ 2.20 GHz (4 CPUs), ~2.2 GHz, RAM: 3 GB, 32-bit OS.

4 Results and Discussion

In this section, we present the energy conservation error and running time results for each variation of the method. As mentioned in the previous section, we have 15 scenarios where we vary the total length and the step size for each of the 4 variations of the nonlinearity parameter. The results of these simulations are presented in Tables 4 to 7, which will be discussed next.

In Table 5, we present the results for the 15 scenarios with the nonlinearity parameter set at zero, whereas γ = 110^{-3}, 1010^{-3} and 10010^{-3} W^{-1}/km are presented in Tables 4, 5, 6 and 7, respectively. Although the tables show the results obtained from the simulations on a desktop computer, the results obtained when tested on a laptop kept the same proportions, with slight differences in the results due to their difference of computational power.

From Table 4 we can see that the difference between the running time of the symmetrized approach and the running time of the other approaches varies from 50% in scenario 7 up to around 86% in scenario 4. In Table 5 the smallest difference is 54% in scenario 11, and the largest one is 126% in scenario 8. Similarly, in Table 6 we have differences of 55% up to 101%, and in Table 7, it varies from 57% up to 115%. Thus, in the case where the parameter γ is zero, the computation time is smaller, which shows that the nonlinear effects require some extra computational effort that affects the running time. Regarding the energy conservation error, we see similar results in most scenarios for both N-D and Symmetrized variations, although it is expected that the Symmetrized approach is always better.

In Tables 4, 5 and 6, in scenarios where the propagated distance is longer than 1 km, there is an error in the energy conservation significantly greater than in the previous scenarios, increasing from the order of 10^{-11}, in the worst cases of 1 km, to values in the order of 10^{-4} to 10^{-2}. This is due to the longer propagated distance, which causes a greater dispersion in the signal and thus causes the pulse to exceed the width of the time window. Therefore, part of the energy is not considered in the final pulse energy calculations.

In Table VII there is no such difference regarding the distance propagated since the high nonlinearity of γ = 10010^{-3} causes significant distortions even for short distances, thus maintaining errors of the order of 10^{-4} to 10^{-2} for all input values.

By comparing the results from the four tables, we also observe that the symmetrized approach does not always present the best results regarding energy conservation, as we can see in all scenarios of Table 4 and in the first scenarios of the other tables. From this, we believe that the presence of the nonlinearity parameter and the propagated distance have direct influence on the advantages of the symmetrized approach.

From all tables we realize that N-D and D-N variations have a very similar running time, always in the same order of magnitude, which denotes there is no advantage between these variations. We can even state that the D-N approach presents better results in most scenarios. Thus, we can conclude that both variations can be implemented once they present similar computational cost. On the other hand, the Symmetrized method shows, as expected, a running time higher than the other variations, which is due to its extra amount of calculations.

Additionally, Figures 3, 4, 5 and 6 show the shape of the initial pulse (blue lines) and the final pulse (red dashed lines) for different scenarios where we varied the value of the nonlinearity coefficient (γ) and the distance traveled by the pulse. We emphasize that, in all cases, it is expected that the pulse energy is conserved during their propagation, since we are not considering loss (α = 0). Thus, the area of the final pulse must always be the same as the initial pulse, which was proven by means of simulations.

In Figures 3(a) and 3(b), we do not consider nonlinear effects (γ = 0). Thus, we observe only group velo-

Table 4: Results for the different scenarios with $\gamma = 0$.

Input parameters				Energy conservation error		Running time (s)		
Scenario	**L (km)**	**h (m)**	**S**	**N-D**	**Symmetrized**	**N-D**	**D-N**	**Symmetrized**
1	1	100	10	-1.21E-13	-2.78E-13	5.39E-03	5.16E-03	8.73E-03
2	1	20	50	-6.59E-13	-1.34E-12	2.53E-02	2.46E-02	4.11E-02
3	1	10	100	-1.34E-12	-2.55E-12	4.97E-02	4.79E-02	8.03E-02
4	**1**	**2**	**500**	**-5.99E-12**	**-1.12E-11**	**2.33E-01**	**3.29E-01**	**3.84E-01**
5	1	1	1000	-1.12E-11	-2.44E-11	5.39E-01	4.50E-01	7.84E-01
6	10	1000	10	1.10E-03	1.10E-03	5.13E-03	4.89E-03	8.97E-03
7	**10**	**200**	**50**	**1.10E-03**	**1.10E-03**	**2.53E-02**	**2.45E-02**	**4.88E-02**
8	10	100	100	1.10E-03	1.10E-03	6.23E-02	4.79E-02	8.05E-02
9	10	20	500	1.10E-03	1.10E-03	2.30E-01	2.31E-01	3.92E-01
10	10	10	1000	1.10E-03	1.10E-03	4.75E-01	5.50E-01	7.87E-01
11	50	5000	10	7.20E-03	7.20E-03	6.12E-03	5.86E-03	1.00E-02
12	50	1000	50	7.20E-03	7.20E-03	2.60E-02	2.54E-02	4.20E-02
13	50	500	100	7.20E-03	7.20E-03	4.87E-02	4.95E-02	8.13E-02
14	50	100	500	7.20E-03	7.20E-03	2.34E-01	3.09E-01	3.94E-01
15	50	50	1000	7.20E-03	7.20E-03	4.60E-01	4.56E-01	7.93E-01

Table 5: Results for the different scenarios with $\gamma = 1 \times 10^{-3} W^{-1}/km$.

Input parameters				Energy conservation error		Running time (s)		
Scenario	**L (km)**	**h (m)**	**S**	**N-D**	**Symmetrized**	**N-D**	**D-N**	**Symmetrized**
1	1	100	10	-1.21E-13	-2.43E-13	5.81E-03	6.45E-03	1.00E-02
2	1	20	50	-6.42E-13	-1.23E-12	2.68E-02	2.62E-02	4.27E-02
3	1	10	100	-1.27E-12	-2.36E-12	5.15E-02	7.07E-02	8.27E-02
4	1	2	500	-5.93E-12	-1.12E-11	2.55E-01	2.51E-01	4.07E-01
5	1	1	1000	-1.14E-11	-2.36E-11	5.01E-01	5.29E-01	9.06E-01
6	10	1000	10	4.80E-03	4.90E-03	5.51E-03	6.80E-03	1.01E-02
7	10	200	50	7.34E-04	4.43E-04	2.77E-02	2.81E-02	4.34E-02
8	**10**	**100**	**100**	**5.97E-04**	**5.05E-04**	**1.05E-01**	**5.37E-02**	**8.35E-02**
9	10	20	500	5.69E-04	5.57E-04	2.51E-01	2.59E-01	4.15E-01
10	10	10	1000	5.69E-04	5.63E-04	5.01E-01	5.67E-01	8.26E-01
11	**50**	**5000**	**10**	**4.90E-03**	**5.40E-03**	**5.34E-03**	**6.67E-03**	**9.95E-03**
12	50	1000	50	4.10E-03	8.30E-03	2.72E-02	2.70E-02	4.42E-02
13	50	500	100	7.80E-03	1.26E-02	5.40E-02	5.49E-02	9.61E-02
14	50	100	500	9.60E-03	1.04E-02	2.59E-01	2.54E-01	4.22E-01
15	50	50	1000	9.70E-03	1.01E-02	4.95E-01	5.07E-01	8.86E-01

city dispersion with the pulse losing altitude (maximum amplitude) and being enlarged in the time domain. We notice that for a distance of 10 km, the dispersion is much more intense, since it is, in fact, proportional to the distance propagated. The energy difference of the two pulses was from the order of 10^{-11} and 10^{-3}, respectively.

In Figures 4(a) and 4(a), we consider nonlinear effects from the order of $\gamma = 1 \times 10^{-3}$ W^{-1}/km. Thus, the nonlinear effect of SPM acts on the pulse modifying its amplitude in high power points, which produces a narrowing caused by the fact the SPM overcomes the dispersion caused by the linear effect of GVD. We observe that for a distance of 10 km the dispersion is more intense, with a smaller narrowing of the pulse, whose maximum value falls from 1.9 W at 1 km to 1.2 W at 10 km. The difference between the total energy of the initial and final pulses in the two scenarios was also from

Table 6: Results for the different scenarios with $\gamma = 10 \times 10^{-3}\ W^{-1}/km$.

Input parameters				Energy conservation error		Running time (s)		
Scenario	**L (km)**	**h (m)**	**S**	**N-D**	**Symmetrized**	**N-D**	**D-N**	**Symmetrized**
1	1	100	10	-1.39E-13	-2.60E-13	5.82E-03	5.76E-03	8.63E-03
2	1	20	50	-6.42E-13	-1.16E-12	2.62E-02	3.28E-02	4.45E-02
3	1	10	100	-1.23E-12	-2.41E-12	5.20E-02	5.24E-02	8.19E-02
4	1	2	500	-6.02E-12	-1.08E-11	2.48E-01	2.61E-01	3.93E-01
5	1	1	1000	-1.07E-11	-2.35E-11	4.86E-01	5.38E-01	7.96E-01
6	10	1000	10	2.14E-02	8.10E-03	6.01E-03	6.81E-03	9.20E-03
7	**10**	**200**	**50**	**1.30E-03**	**6.44E-04**	**4.50E-02**	**2.69E-02**	**4.44E-02**
8	10	100	100	5.20E-04	2.60E-03	5.37E-02	6.89E-02	8.64E-02
9	10	20	500	4.19E-05	1.24E-04	3.22E-01	2.62E-01	4.18E-01
10	10	10	1000	5.84E-05	8.06E-05	5.41E-01	5.13E-01	8.50E-01
11	50	5000	10	2.70E-03	1.58E-02	6.40E-03	7.15E-03	9.87E-03
12	50	1000	50	6.60E-03	3.98E-02	2.87E-02	2.76E-02	4.53E-02
13	50	500	100	3.60E-03	1.80E-03	6.64E-02	5.50E-02	8.31E-02
14	**50**	**100**	**500**	**1.91E-02**	**1.50E-03**	**2.61E-01**	**2.65E-01**	**4.73E-01**
15	50	50	1000	4.40E-03	7.38E-02	5.96E-01	5.44E-01	8.39E-01

Table 7: Results for the different scenarios with $\gamma = 100 \times 10^{-3}\ W^{-1}/km$.

Input parameters				Energy conservation error		Running time (s)		
Scenario	**L (km)**	**h (m)**	**S**	**N-D**	**Symmetrized**	**N-D**	**D-N**	**Symmetrized**
1	1	100	10	4.80E-03	5.63E-04	6.32E-03	5.94E-03	8.35E-03
2	1	20	50	4.10E-03	1.07E-02	2.81E-02	2.90E-02	4.35E-02
3	1	10	100	7.50E-03	2.51E-02	5.38E-02	5.26E-02	8.76E-02
4	1	2	500	9.08E-05	5.10E-03	2.61E-01	3.38E-01	4.18E-01
5	**1**	**1**	**1000**	**1.10E-07**	**1.20E-03**	**5.25E-01**	**5.34E-01**	**9.17E-01**
6	10	1000	10	1.14E-02	1.03E-02	8.07E-03	7.09E-03	9.30E-03
7	10	200	50	5.80E-03	2.81E-02	3.02E-02	2.63E-02	4.61E-02
8	**10**	**100**	**100**	**5.20E-02**	**7.05E-04**	**9.85E-02**	**5.34E-02**	**8.55E-02**
9	10	20	500	3.60E-03	9.17E-04	2.63E-01	2.61E-01	4.47E-01
10	10	10	1000	1.61E-02	8.33E-04	5.11E-01	5.62E-01	8.76E-01
11	50	5000	10	6.50E-03	4.66E-02	6.92E-03	6.42E-03	1.14E-02
12	50	1000	50	1.62E-02	2.40E-03	3.14E-02	3.06E-02	4.63E-02
13	50	500	100	9.70E-03	1.20E-03	5.64E-02	5.60E-02	9.08E-02
14	50	100	500	4.18E-02	1.30E-02	2.68E-01	2.66E-01	4.31E-01
15	50	50	1000	8.50E-03	3.30E-03	6.01E-01	5.16E-01	8.74E-01

the order of 10^{-11} and 10^{-3}, respectively.

In figures 5(a) and 5(b), we fix gamma at $\gamma = 10\times10^{-3}$ W^{-1}/km. We realize that the SPM acts more intensively on the pulse. For 1 km it generates three peaks (one central and two symmetrical by the sides), with the side peaks reaching maximum power of 1.3 W, whereas for 10 km it presents a central peak and several small peaks, with power lower than 0.1 W.

In Figures 6(a) and 6(b), we fix gamma at $\gamma = 100\times10^{-3}$ W^{-1}/km. We observe that the SPM creates new peaks at 1 km and makes the pulse unintelligible at 50 km.

5 Conclusion

By comparing the three variations of the Split-Step Fourier method implemented in this paper to simulate the propagation of an ultrashort pulse under dispersive

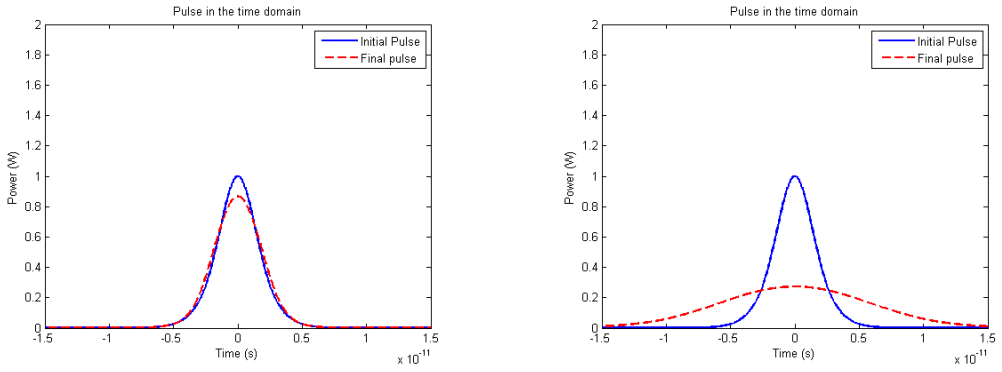

(a) (b)

Figure 3: Initial pulse and final pulse for γ = 0 W^{-1}/km after a distance of (a) 1 km; (b) 10 km.

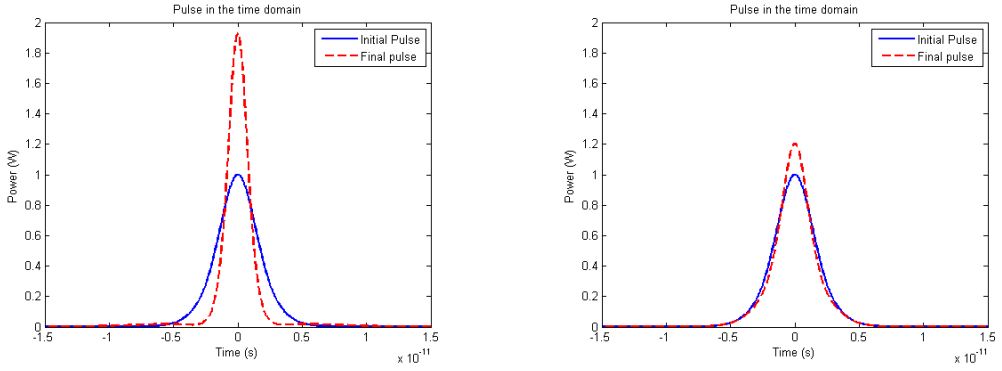

(a) (b)

Figure 4: Initial pulse and final pulse for $\gamma = 1 \times 10^{-3}\ W^{-1}$/km after a distance of (a) 1 km; (b) 10 km.

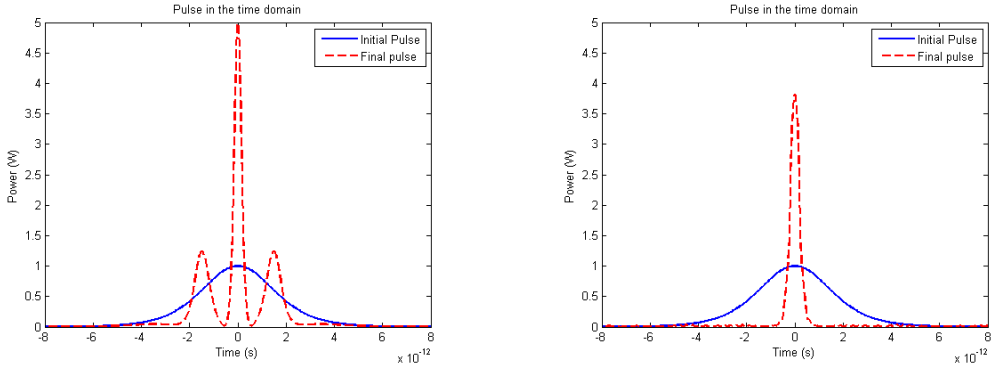

(a) (b)

Figure 5: Initial pulse and final pulse for $\gamma = 10 \times 10^{-3}\ W^{-1}$/km after a distance of (a) 1 km; (b) 10 km.

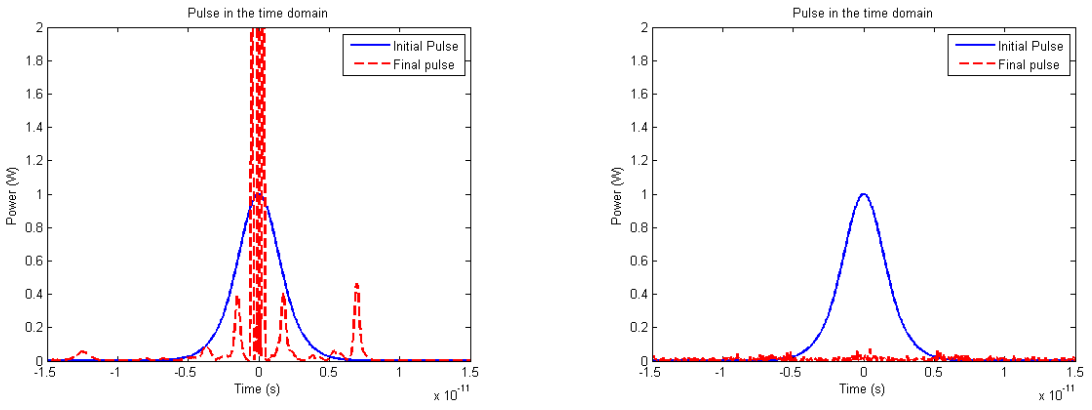

(a) (b)

Figure 6: Initial pulse and final pulse for $\gamma = 100 \times 10^{-3}\ W^{-1}$/km after a distance of (a) 1 km; (b) 10 km.

and nonlinear effects, we conclude that the N-D variations (first nonlinear effects and then the dispersive one), D-N (first the dispersive effects and then the nonlinear effects) and Symmetrized approaches are simple to implement and computationally efficient.

Regarding the computational time, we observe that the N-D and D-N variations take almost the same time, with no consistent advantages of these variations over the other. However, both N-D and D-N variations are faster than the symmetrized approach, with differences that can reach up to 126%, depending on the length propagated.

As to energy conservation, we realize that in all cases the energy is conserved as expected, since we do not consider losses (α = 0). However, there is an error in energy conservation precision generated computationally, which varied from 10^{-13} to 10^{-2}, depending on the scenario investigated. This error increases as the propagated distance increases, since the dispersive effects are proportional to the distance and make the pulse tail exceed the time window in some cases. Nonlinear effects also have a slight influence on this error, especially when the window is not large enough.

Although the literature states that the time window width must be 10 to 20 times greater than the time width of the initial pulse (KEISER, 2000), our tests show that these proportions can generate errors in the pulse energy conservation from the order of 10^{-2}. We conclude that a time window 100 times greater than the width of the initial pulse provides the best results for energy conservation, with errors that remain in the order of 10^{-11} regardless of the value of γ for a distance of 1 km. For a distance from 10 km, we suggest working with a window 500 times greater than the initial pulse.

In future works we will investigate the performance of the different variations of the symmetrized approach (D-N-D and N-D-N), refine the error calculation, and also observe the behavior of the method under the influence of others nonlinear effects, and also do a deeper study on the influence of the time window.

Acknowledgments

We thank CAPES, CNPq, and FUNCAP for financial support through scholarships that allowed the completion of this work.

References

AGRAWAL, G. P. **Nonlinear Fiber Optics**. 3rd. ed. San Diego, USA: Academic Press, 2001.

BALAC, S.; FERNANDEZ, A. Mathematical analysis of adaptive step-size techniques when solving the nonlinear schrödinger equation for simulating light-wave propagation in optical fibers. **Optics Communications**, Elsevier, v. 329, n. 1, p. 1–9, 2014.

BALAC, S.; MAHÉ, F. An embedded split-step method for solving the nonlinear schrödinger equation in optics. **Journal of Computational Physics**, Elsevier, v. 280, n. 1, p. 295–305, 2015.

BAYINDIR, C. Compressive split-step fourier method. **Journal of Applied and Engineering Mathematics**,

Turkic World Mathematical Society, v. 5, n. 2, p. 298–307, 2015.

DUO, S.; ZHANG, Y. Mass-conservative fourier spectral methods for solving the fractional nonlinear schrödinger equation. **Computers & Mathematics with Applications**, Elsevier, v. 71, n. 11, p. 2257–2271, 2016.

GROSZ, D. **Efeitos não lineares em sistemas de comunicação óptica de longas distâncias e altas taxas**. Tese (Doutorado em Física) — Instituto de Física da Unicamp, Campinas, 1998.

KEISER, G. **Optical Fibers Communications**. 3rd. ed. USA: McGraw-Hill, 2000.

KOMNINOS, P. G. **Análise da dinâmica do funcionamento de lasers de fibra dopada com érbio sob a óptica da equação de Ginzburg-Landau**. Tese (Masters in Electrical Engineering) — Universidade Presbiteriana Mackenzie, São Paulo, 2010.

LIN, C.-Y.; ASIF, R.; HOLTMANNSPOETTER, M.; SCHMAUSS, B. Step-size selection for split-step based nonlinear compensation with coherent detection in 112-gb/s 16-qam transmission. **Chinese Optics Letters**, Chinese Optical Society, v. 10, n. 2, p. 020605, 2012.

LIU, X. Adaptive higher-order split-step fourier algorithm for simulating lightwave propagation in optical fiber. **Optics Communications**, Elsevier, v. 282, n. 7, p. 1435–1439, 2009.

MUSLU, G. M.; ERBAY, H. Higher-order split-step fourier schemes for the generalized nonlinear schrödinger equation. **Mathematics and Computers in Simulation**, Elsevier, v. 67, n. 6, p. 581–595, 2005.

RIBEIRO, J. A. J. **Comunicações Ópticas**. 4. ed. São Paulo: Saraiva, 2003.

SHAO, J.; LIANG, X.; KUMAR, S. Comparison of split-step fourier schemes for simulating fiber optic communication systems. **IEEE Photonics Journal**, IEEE, v. 6, n. 4, p. 7200515, 2014.

____. An efficient scheme of split-step fourier method for fiber optic communication systems. In: INTERNATIONAL SOCIETY FOR OPTICS AND PHOTONICS. **Photonics North 2014**. Montréal, Canada, 2014. v. 9288, p. 928806.

TAYLOR, L. **A comparison between the Split Step Fourier and Finite-Difference method in analysing the soliton collision of a type of Nonlinear Schrödinger equation found in the context of optical pulses**. TWMS, 2015.

WASHBURN, B. **Numerical Solutions to the nonlinear Schrödinger Equation. (Thesis)**. Atlanta, GA, 2002. 134–157 p.

ZHANG, J.; LI, X.; DONG, Z. Digital nonlinear compensation based on the modified logarithmic step size. **Journal of Lightwave Technology**, IEEE, v. 31, n. 22, p. 3546–3555, 2013.

ZHANG, Q.; HAYEE, M. I. Symmetrized split-step fourier scheme to control global simulation accuracy in fiber-optic communication systems. **Journal of Lightwave Technology**, IEEE, v. 26, n. 2, p. 302–316, 2008.